Electron-impact excitation from metastable helium: $2\,^{1,3}S \rightarrow n\,^{1,3}L$ $(L=0, 1, 2; n=2,...,\infty)$

D. C. Cartwright and G. Csanak
Theoretical Division, Los Alamos National Laboratory, Los Alamos, New Mexico 87545
(Received 16 August 1996)

Integral cross sections for electron-impact excitation from the helium $2\,^3S$ and $2\,^1S$ metastable excited states, to all energetically higher S, P, and D excited states, are reported from threshold to 200 eV. These cross sections have been obtained using the distorted-wave approximation, and are compared to other experimental and theoretical results. Special attention is paid to obtaining an adequate representation for the wave functions of the $n\,^1S$ excited states ($n=2$, 3, and 4). The total integral electronic excitation cross sections from each of these metastable states, summed over n for fixed L of the final state, and then summed over L, are also reported. These results are combined with other cross-section data to obtain the total inelastic integral cross section for inelastic electron scattering from each of these two helium metastable states. [S1050-2947(97)08102-X]

PACS number(s): 34.50.Fa

I. INTRODUCTION

In a series of papers [1–3], results from first-order many-body theory (FOMBT) and the distorted-wave (DW) approximation have been reported for differential cross sections (DCS's) and integral cross sections (ICS's) for the electron-impact excitation from the ground ($1\,^1S$) state, $2\,^3S$, and $2\,^1S$ metastable excited states of helium to excited states with $n=2$ and 3. The present work extends these earlier results for excitation from the $2\,^{1,3}S$ metastable excited states to obtain cross sections to S, P, and D excited states with $n\geqslant 4$, and to obtain the total integral excitation cross section (summed over all n). ICS's for the excitation from the $2\,^1S$ metastable state of helium to $n\,^1S$ levels ($n=3$ and 4), which were not reported previously, are reported here and compared with recent experimental and theoretical results.

II. THEORY

The theoretical foundation of FOMBT, both for excitation from the ground state [4] and for excitation from excited states [5], has been reported previously, as well as the specific implementation of FOMBT and the DW approximation for the helium target [1–3]. It was also shown recently [5] how the DW approximation for excitations out of the metastable states can be obtained by selectively summing (up to infinite order) a set of diagrams describing the interaction of the scattering electron with the initial and final states of the target. Consequently, this paper will report only the extension of those previous studies.

Density matrix for $2\,^1S \rightarrow n\,^1S$ $(n=3, 4,...)$ transitions

The calculation of the excited-state to excited-state transition density matrix for $2\,^1S \rightarrow n\,^1S$ $(n=3,4,...)$ transitions is discussed in detail here because the radial wave functions used in the computations for the $n\,^1S$ $(n\geqslant 2)$ states of helium need to be generated with some care. These $n\,^1S$ states require more attention than the other states of helium in order to obtain an accurate, but still computationally tractable, representation because they are of the same symmetry as the ground state.

For $2\,^1S \rightarrow n\,^1S$ $(n\geqslant 3)$ transitions, the transition density matrices were obtained using the Cohen-McEachran wave functions in the form [6,7]

$$\Psi_{\overline{n^1}LM_L}(x_1,x_2)=N_{\overline{nL}}[\varphi_0(\mathbf{r}_1)\varphi_{\overline{nL}M_L}(\mathbf{r}_2) + \varphi_0(\mathbf{r}_2)\varphi_{\overline{nL}M_L}(\mathbf{r}_1)]\frac{1}{\sqrt{2}}[\alpha(\sigma_1)\beta(\sigma_2) - \beta(\sigma_1)\alpha(\sigma_2)], \tag{1}$$

where $\varphi_0(\mathbf{r})$ is the He^+ $1s$ normalized orbital (fixed core), which is (in atomic units)

$$\varphi_0(\mathbf{r})=2^{5/2}e^{-2r}Y_{00}(\hat{r}), \tag{2}$$

and the $\varphi_{\overline{nL}M_L}(\mathbf{r})$ orbitals are obtained by solving the fixed-core Hartree-Fock equations, and the $\varphi_{\overline{nL}M_L}(\mathbf{r})$ orbitals are assumed to be normalized according to

$$\int |\varphi_{\overline{nL}M_L}(\mathbf{r})|^2 d\mathbf{r}=1. \tag{3}$$

In order for the wave function $\Psi_{\overline{nL}M_L}(x_1,x_2)$ to be similarly normalized according to

$$\int |\Psi_{\overline{nL}M_L}(x_1,x_2)|^2 dx_1 dx_2=1, \tag{4}$$

the normalization constant in Eq. (1) must be

$$N_{\overline{nL}}=[2(1+|S_{\overline{nL},0}|)^2]^{-1/2}, \tag{5}$$

where

$$S_{\overline{nL},0}=\int d\mathbf{r}\ \varphi^*_{\overline{nL}M_L}(\mathbf{r})\varphi_0(\mathbf{r}) \tag{6}$$

is the customary overlap integral.

The transition density matrix between states $m=\overline{mL}^m M_L^m$ and $n=\overline{nL}^n M_L^n$, using the representation given by Eq. (1) for both wave functions, and assuming that both are singlet states, is given by [5]

$$
\begin{aligned}
X_{m,n}(x,x') &\equiv 2\int \Psi^*_m(x,x_2)\Psi_n(x',x_2)\,dx_2 \\
&= N_{\overline{mL}^m} N_{\overline{nL}^n} 2\int d\mathbf{r}_2[\varphi^*_0(\mathbf{r})\varphi^*_{\overline{mL}^m M_L^m}(\mathbf{r}_2)+\varphi^*_0(\mathbf{r}_2)\varphi^*_{\overline{mL}^m M_L^m}(\mathbf{r})][\varphi_0(\mathbf{r}')\varphi_{\overline{nL}^n M_L^n}(\mathbf{r}_2)+\varphi_0(\mathbf{r}_2)\varphi_{\overline{nL}^n M_L^n}(\mathbf{r}')] \\
&\quad\times\int d\sigma_2[\alpha(\sigma)\beta(\sigma_2)-\beta(\sigma)\alpha(\sigma_2)][\alpha(\sigma')\beta(\sigma_2)-\beta(\sigma')\alpha(\sigma_2)] \\
&= N_{\overline{mL}^m} N_{\overline{nL}^n}\Bigg[\int d\mathbf{r}_2\varphi^*_0(\mathbf{r}_2)\varphi_{\overline{nL}^n M_L^n}(\mathbf{r}_2)\varphi^*_{\overline{mL}^m M_L^m}(\mathbf{r})\varphi_0(\mathbf{r}')+\int d\mathbf{r}_2\varphi^*_{\overline{mL}^m M_L^m}(\mathbf{r}_2)\varphi_0(\mathbf{r}_2)\varphi^*_0(\mathbf{r})\varphi_{\overline{nL}^n M_L^n}(\mathbf{r}') \\
&\quad+\varphi^*_{\overline{mL}^m M_L^m}(\mathbf{r})\varphi_{\overline{nL}^n M_L^n}(\mathbf{r}')\Bigg][\alpha(\sigma)\alpha(\sigma')+\beta(\sigma)\beta(\sigma')] \\
&\equiv N_{\overline{mL}^m} N_{\overline{nL}^n}[S_{0,n}\varphi_{\overline{mL}^m M_L^m}(\mathbf{r})\varphi_0(\mathbf{r}')+S_{m,0}\varphi^*_0(\mathbf{r})\varphi_{\overline{nL}^n M_L^n}(\mathbf{r}')+\varphi^*_{\overline{mL}^m M_L^m}(\mathbf{r})\varphi_{\overline{nL}^n M_L^n}(\mathbf{r}')] \\
&\quad\times[\alpha(\sigma)\alpha(\sigma')+\beta(\sigma)\beta(\sigma')] \\
&\equiv X_{m,n}(\mathbf{r},\mathbf{r}')[\alpha(\sigma)\alpha(\sigma')+\beta(\sigma)\beta(\sigma)], \qquad (7)
\end{aligned}
$$

where the definitions of $S_{0,n}$ and $S_{m,0}$ are analogous to Eq. (6).

The spatial part of the transition density matrix is

$$
\begin{aligned}
X_{m,n}(\mathbf{r},\mathbf{r}') &= N_{\overline{mL}^m} N_{\overline{nL}^n}[\varphi^*_{\overline{mL}^m M_L^m}(\mathbf{r})\varphi_{\overline{nL}^n M_L^n}(\mathbf{r}') \\
&\quad+S_{0,n}\varphi^*_{\overline{mL}^m M_L^m}(\mathbf{r})\varphi_0(\mathbf{r}') \\
&\quad+S_{m,0}\varphi^*_0(\mathbf{r})\varphi_{\overline{nL}^n M_L^n}(\mathbf{r}')]. \qquad (8)
\end{aligned}
$$

For excitation from an $m\ ^1S$ state to an $n\ ^1S$ state $[L^m=L^n=M_L^m\equiv M_L^n=0]$, Eq. (8) becomes

$$
\begin{aligned}
X_{m,n}(\mathbf{r},\mathbf{r}') &= N_{\overline{mS}} N_{\overline{nS}}[\varphi^*_{\overline{mS}}(\mathbf{r})\varphi_{\overline{nS}}(\mathbf{r}')+S_{0,n}\varphi^*_{\overline{mS}}(\mathbf{r})\varphi_0(\mathbf{r}') \\
&\quad+S_{m,0}\varphi^*_0(\mathbf{r})\varphi_{\overline{nS}}(\mathbf{r}')], \qquad (9)
\end{aligned}
$$

which does not have a simple form of a product of one-electron orbitals. However, one can obtain a simple product form, to a good approximation, as follows:

(1) If one of the states is highly excited, (e.g., $\overline{n}\gg 1$) then $S_{0,n}\approx 0$, and, to a good approximation, Eq. (9) becomes

$$
\begin{aligned}
X_{m,n}(\mathbf{r},\mathbf{r}') &= N_{\overline{mS}} N_{\overline{nS}}[\varphi^*_{\overline{mS}}(\mathbf{r})\varphi_{\overline{nS}}(\mathbf{r}')+S_{m,0}\varphi^*_0(\mathbf{r})\varphi_{\overline{nS}}(\mathbf{r}')] \\
&= N_{\overline{mS}} N_{\overline{nS}}[\varphi^*_{\overline{mS}}(\mathbf{r})+S_{m,0}\varphi^*_0(\mathbf{r})]\varphi_{\overline{nS}}(\mathbf{r}). \qquad (10)
\end{aligned}
$$

(2) if both $\overline{m}$ and $\overline{n}$ are >1 (which is the present situation), then to a good approximation $S_{0,n}S_{m,0}\approx 0$, and Eq. (9) becomes

$$
\begin{aligned}
&X_{m,n}(\mathbf{r},\mathbf{r}') \\
&\quad= N_{\overline{mS}} N_{\overline{nS}}[\varphi^*_{\overline{m}}(\mathbf{r})+S_{m,0}\varphi^*_0(\mathbf{r})][\varphi_{\overline{nS}}(\mathbf{r}')+S_{0,n}(\mathbf{r}')]. \qquad (11)
\end{aligned}
$$

Equations (10) and (11) are in the desired factored form as the product of ''one-electron'' orbitals, which is substantially easier to use computationally than Eq. (9) while still being a very good approximation to it.

III. RESULTS AND DISCUSSION

A. $2\ ^1S\rightarrow n\ ^1L$ ($n=3, 4$; $L=0, 1, 2$) excitations

Because the cross sections involving $n\ ^1S$ initial and/or final excited states are sensitive to details of the specific wave functions used, various generalized oscillator strengths (GOS's) from our transition density [Eqs. (7) and (11)] have been calculated and compared with results from Kim and Inokuti [8], who used highly correlated wave functions. These GOS results for the $2^1S\rightarrow n\ ^1P$ ($n=2$ and 3) and for the $2\ ^1S\rightarrow 3\ ^1S$, $3\ ^1D$ transitions are shown in Fig. 1. The comparisons in Fig. 1 suggests that the transition density employed in this study for the $n\ ^1S$ states utilizing the factored form for the $n\ ^1S$ wave functions is a reasonably good approximation to the exact transition density.

In order to highlight the effect of different wave functions for the $2\ ^1S$ and $2\ ^3S$ states of helium (which differ only in the orientation of the electron spin in the excited state orbital relative to that in the ground-state orbital), Fig. 2 shows a comparison of our DW approximation DCS results for the $2\ ^3S\rightarrow 3\ ^3S$ and $3\ ^3P$ excitations with that for the $2\ ^1S\rightarrow 3\ ^1S$ and $3\ ^1P$ excitations, at 20- and 50-eV incident electron energies. This comparison shows a big difference in the DCS's for scattering angles greater than 40°, and suggests that a small difference in the spatial portions of the excited $n\ ^1S$ and $n\ ^3S$ wave functions can have a big effect on the DCS's for excitation from these lowest two excited states. It should be noted here that the ICS's, which are determined primarily by the strong forward scattering peaks in the DCS's, are not expected to show the sensitivity predicted for the DCS's.

The only experimental data presently available against which the predictions in Fig. 2 can be compared are those of Müller-Fiedler *et al.* [9] for the $2\ ^3S\rightarrow 3\ ^3S$, $3\ ^3P$ transitions. A comparison with the DCS's predicted by the DW approximation employed here for excitation from the $2\ ^3S$ state has been made by Cartwright and Csanak [3], and the agreement in shape was found to be nearly quantitative over the limited range in scattering angle for the experiment. Unfortunately, there are presently no DCS measurements for scattering angles $\geqslant 40°$ against which the predictions in Fig. 2 can be

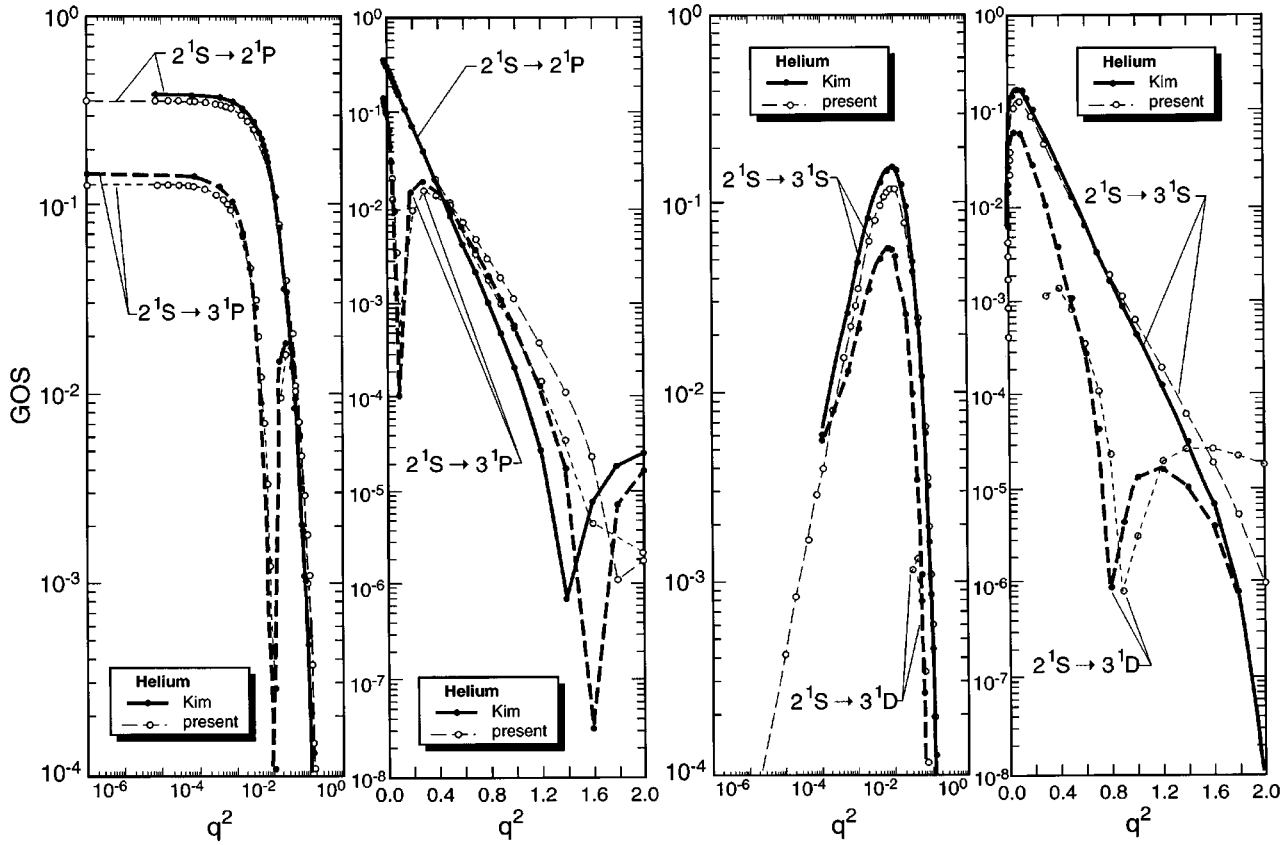

FIG. 1. Comparison of present generalized oscillator strengths (GOS) (light lines with open symbols) with those of Kim and Inokuti [8] (heavy lines with closed symbols) for (i) the $2\,^1S \rightarrow 2\,^1P$, $3\,^1P$ transitions (two left panels), and (ii) for the $2\,^1S \rightarrow 3\,^1S$, $3\,^1D$ transitions (two right panels), in helium. The first and third panels (from the left) are logarithmic in the independent variable (q^2), and the second and fourth panels are linear in (q^2), the second and fourth panels are linear in q^2. Both logarithmic and linear representations are shown because they emphasize different regions of the GOS.

compared which is the region where the greatest variations with incident electron energy occur. In addition, there are no experimental DCS data for excitation from the $2\,^1S$ state, for any electron scattering angle, to determine if the DCS's for excitation from the $2\,^1S$ state are indeed substantially smaller than the corresponding transitions from the $2\,^3S$ state for scattering angles greater than 40°, as is shown in Fig. 2.

The DW approximation results for the $2\,^1S \rightarrow n\,^1L$ ($n=3$ and 4, and $L=0$, 1, and 2) excitations for the ICS's obtained in this study are shown in Figs. 3 and 4, where they are compared with the experimental results of Lockwood *et al.* [10], with the converged close-coupling (CC) calculations results of Bray and Fursa [11], with the multichannel eikonal theory results of Flannery and McCann [12] and Mansky and Flannery [13], and with the 29-state R-matrix theory calculation results (RM) of Fon, Berrington, and Kingston [14]. The comparisons contained in Figs. 3 and 4 suggest the following conclusions.

(a) Except for the $2\,^1S \rightarrow 3\,^1S$ excitation, the ICS results deduced from the experimental emission cross section data (Lockwood *et al.* [10]) are larger than the corresponding theoretical results. This is expected because the experimental emission cross-section data contain cascade contributions from many higher-lying electronic states, and their contributions are generally difficult to accurately subtract from the emission data in order to obtain a true *direct* excitation cross section to a specific helium excited state.

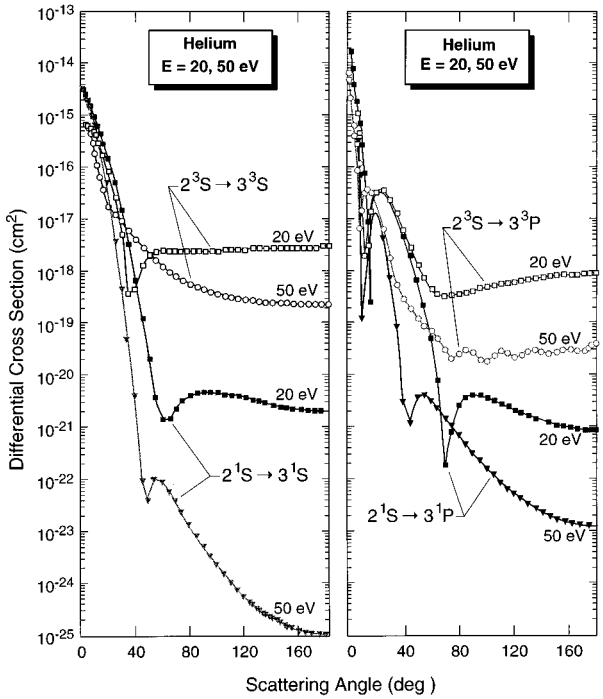

FIG. 2. Comparison of present DW approximation DCS results at 20- and 50-eV incident electron energies for the $2\,^1S \rightarrow 3\,^1S$ transition with that of the $2\,^3S \rightarrow 3\,^3S$ transition (left panel) and for that of the $2\,^1S \rightarrow 3\,^1P$ transition with that of the $2\,^3S \rightarrow 3\,^3P$ transition (right panel), for helium.

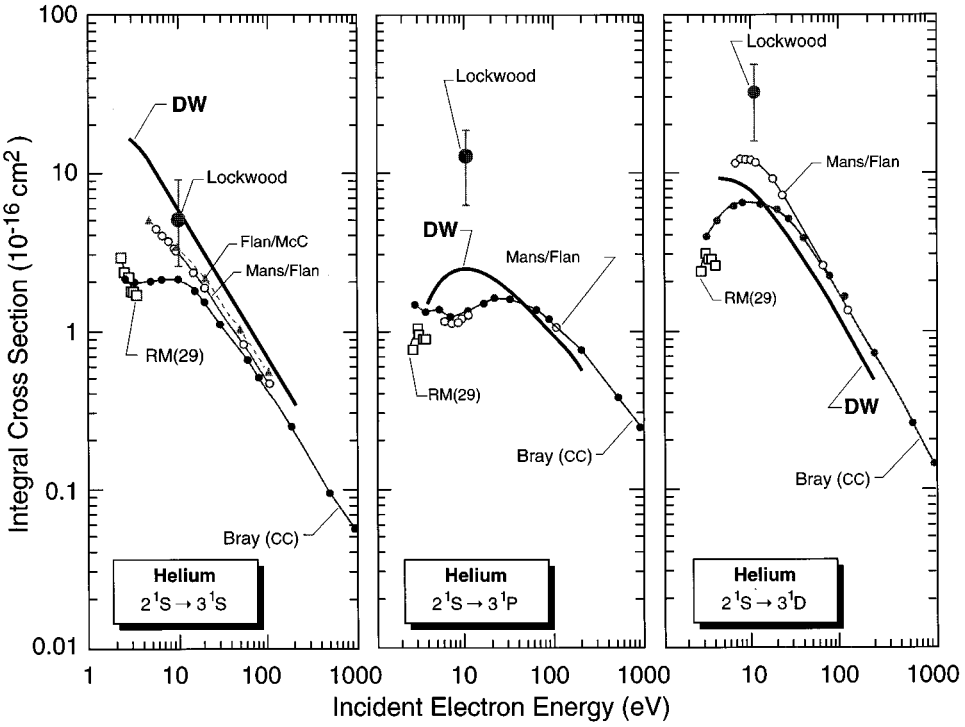

FIG. 3. Comparison of present distorted-wave (DW) approximation ICS results for the $2\,^1S \rightarrow 3\,^1L$ ($L=0$, 1, and 2) electron-impact-induced transitions in helium with the experimental results of Lockwood [10]; with the multichannel eikonal theory results of Flannery and McCann (Flan/McC) [12] and of Mansky and Flannery (Mans/Flan) [13]; with the converged close coupling results of Bray and Fursa [Bray (CC)] [11]; and with the 29-state R-matrix theory results of Fon, Berrington, and Kingston [RM(29)] [14]. Note the large magnitude of these ICS's.

(b) Although over only a small incident electron energy range, the 29-state R-matrix results [RM(29)] of Fon, Berrington, and Kingston [14] are generally in good agreement with the more recent ''converged close coupling'' results (CC) of Bray and Fursa [11], although the agreement is not perfect. These recent CC results of Bray and Fursa [11] appear to be the most complete calculations of inelastic electron scattering by helium reported to date.

(c) The present DW approximation results generally agree well with the CC results of Bray and Fursa [11] for incident electron energies above about 30 eV and are generally larger for energies less than about 30 eV. The fact that the DW approximation predicts a larger ICS at low incident electron energy is expected because the CC method includes second- and higher-order electron-target interactions neglected in the DW approximation, which are expected to be important at low incident electron energies.

(d) It is interesting to note that the DW approximation

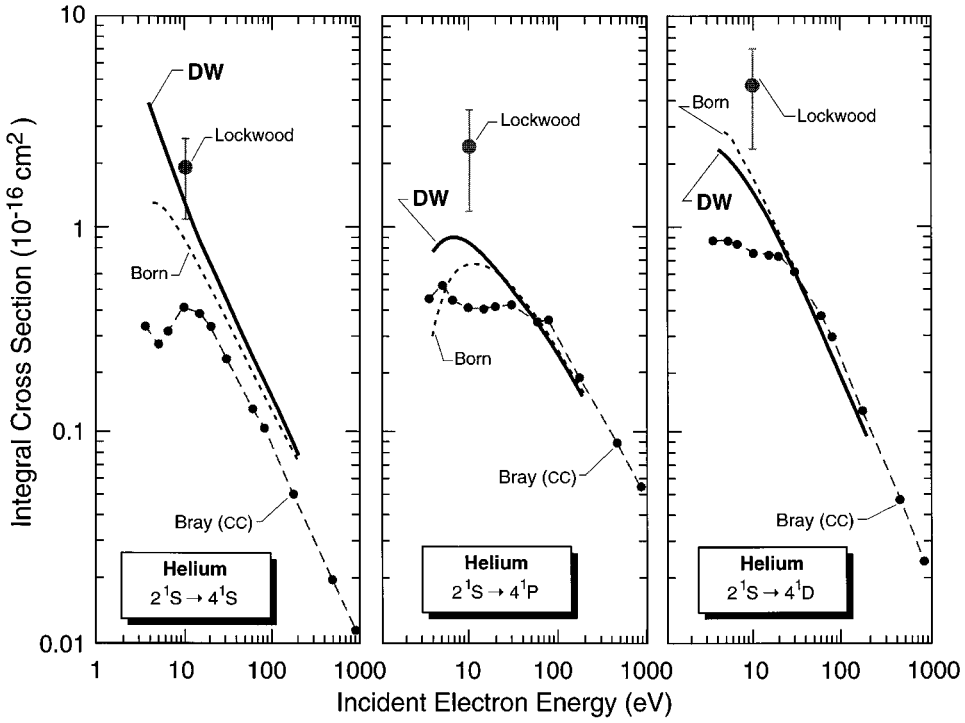

FIG. 4. Same as Fig. 2 except for the $2\,^1S \rightarrow 4\,^1L$ ($L=0$, 1, and 2) transitions. First Born approximation results (Born) obtained in this study are also shown.

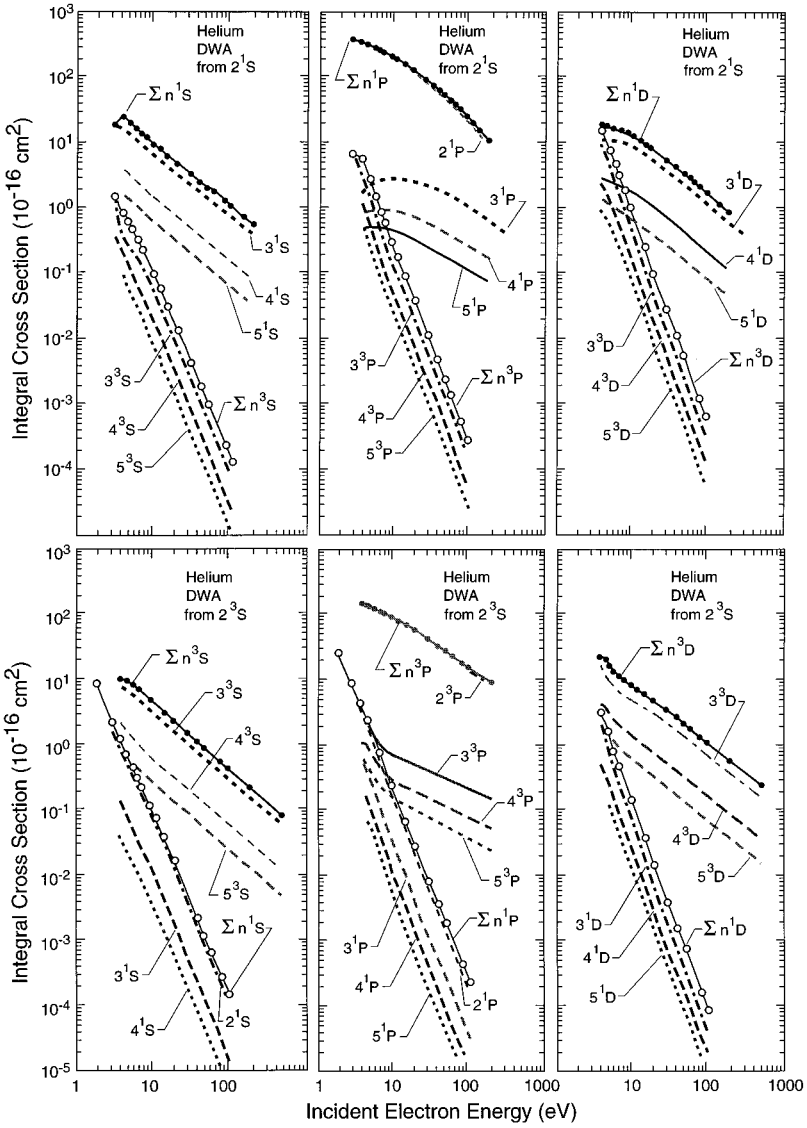

FIG. 5. Present DW approximation ICS results for the $2\,^1S \rightarrow n\,^{1,3}S$ and for the $2\,^3S \rightarrow n\,^{1,3}S$ excitations (left panels), for the $2\,^1S \rightarrow n\,^{1,3}P$ and for the $2\,^3S \rightarrow n\,^{1,3}P$ excitations (center panels), and for the $2\,^1S \rightarrow n\,^{1,3}D$ and for the $2\,^3S \rightarrow n\,^{1,3}D$ excitations (right panels), all for helium and $n=3$, 4, and 5. For all excitations, the sum of the total cross sections for a given initial state to a given L value is also shown at the top of each panel as the heavy curve.

becomes quantitatively accurate for all symmetry final states at about 30 eV and above. At those energies, the difference in magnitudes predicted for the ICS's by the DW and CC models for excitation of the $n\,^1S$ ($n \geqslant 3$) atomic states may be a result of differences in the $n\,^1S$ target wave functions employed in these two studies.

(e) The comparisons with the multi-channel Eikonal (MCE) results of Flannery and McCann [12] and of Mansky and Flannery [13] shown in Fig. 3 suggest that including *only* ''direct channel coupling'' and no electron exchange for electron-impact excitation does not produce reliable ICS's except for dipole-allowed transitions. That is, the MCE approximation neglects all electron-exchange processes in the inelastic electron scattering process, which clearly has a large effect for incident energies less than about 30 eV, and for excitation of excited states which are not dipole connected to the initial state, at all incident electron energies. The MCE approximation is also deficient in that it predicts a zero cross section for the pure exchange transitions (e.g., $2\,^2S \rightarrow n\,^3L$ and for $2\,^3S \rightarrow n\,^1L$).

B. Excitation to higher principal quantum number

Figure 5 contains a summary of the integral cross sections for excitation from the $2\,^{1,3}S$ metastable states of helium to final states with $n=3$, 4, and 5 and for $L=0$, 1, and 2. The upper three panels are for the $2\,^1S$ initial state, the lower three for the $2\,^3S$ initial state. For each of the two rows of three panels, the L value for the final state is 0, 1, and 2 from left to right. Also shown in each of the six panels is the sum of the integral cross sections from a particular initial state ($2\,^1S$ or $2\,^3S$) to all higher electronic states of a given orbital angular momentum symmetry. For example, the upper-left panel shows separately the integral cross sections for $2\,^1S \rightarrow n\,^3S$ and $n\,^1S$ transitions ($n=3$, 4, and 5) and their sum over all n ($n=3, 4, 5, \ldots, \infty$). The sum over all n includes cross sections which were not explicitly calculated but were obtained from the n^{-3} scaling of the cross-section dependence reported previously [1]. For a specific final-state L value, Fig. 5 illustrates how rapidly (with increasing n) the sum of integral cross sections for each initial state converges to the total for each final-state symmetry. It is interesting to

TABLE I. Sum of integral cross sections from $2\,^3S$ state (Å^2).

Energy (eV)	To all $n\,^1S$	To all $n\,^1P$	To all $n\,^1D$	To all $n\,^1L$	To all $n\,^3S$	To all $n\,^3P$	To all $n\,^3D$	To all $n\,^3L$	To all $n\,^{1,3}L$
3.00	2.50+00	1.08+01[a]		1.33+01				2.00+02	2.00+02
4.00	1.41+00	5.17+00	3.09+00	9.67+00	1.18+01	1.83+02	2.13+01	2.16+02	2.13+02
4.50	1.10+00	3.90+00	2.30+00	7.30+00	1.16+01	1.73+02	1.87+01	2.03+02	2.13+02
5.00	8.17−01	2.94+00	1.63+00	5.39+00	1.12+01	1.63+02	1.62+01	1.90+02	1.96+02
6.00	5.29−01	1.80+00	8.13−01	3.14+00	9.38+00	1.46+02	1.28+01	1.68+02	1.71+02
7.00	3.61−01	9.50−01	4.67−01	1.78+00	7.93+00	1.33+02	1.10+01	1.52+02	1.54+02
8.00	2.56−01	6.40−01	3.10−01	1.21+00	6.90+00	1.23+02	9.90+00	1.40+02	1.41+02
10.00	1.40−01	2.82−01	1.41−01	5.63−01	5.39+00	1.07+02	8.34+00	1.21+02	1.21+02
12.00	8.38−02	1.70−01	8.00−02	3.34−01	4.40+00	9.50+01	7.11+00	1.06+02	1.07+02
15.00	4.43−02	7.91−02	3.67−02	1.60−01	3.49+00	8.16+01	6.07+00	9.12+01	9.13+01
20.00	1.91−02	3.27−02	1.43−02	6.60−02	2.60+00	6.64+01	4.78+00	7.38+01	7.39+01
30.00	5.82−03	9.51−03	3.84−03	1.92−02	1.70+00	4.89+01	3.34+00	5.40+01	5.40+01
40.00	2.51−03	3.99−03	1.54−03	8.04−03	1.26+00	3.90+01	2.58+00	4.28+01	4.28+01
50.00	1.28−03	2.04−03	7.63−04	4.08−03	1.00+00	3.25+01	2.09+00	3.55+01	3.55+01
60.00	7.47−04	1.20−03	4.50−04	2.40−03	8.40−01	2.78+01	1.76+00	3.04+01	3.04+01
81.60	2.99−04	4.68−04	1.65−04	9.32−04	6.08−01	2.14+01	1.30+00	2.33+01	2.33+01
100.00	1.62−04	2.54−04	8.79−04	5.04−04	4.95−01	1.81+01	1.06+00	1.96+01	1.96+01
200					2.47−01	1.06+01	5.58−01	1.14+01	1.14+01

[a]$1.08+01 \equiv 1.08\times10^1$.

note that, except for the integral cross sections to $n=2$, the sum of integral cross sections for excitation *from* the $2\,^{1,3}S$ states to a specific L-value final state is largest for $L=2$ (D states). For purposes of completeness, Tables I and II contain the integral cross sections shown in Fig. 5.

Figure 6 shows separately the sums of the integral cross sections for excitation from the $2\,^3S$ (left panel) and $2\,^1S$ (center panel) initial metastable states, to all higher bound states with L values of 0, 1, or 2. The right panel in Fig. 6 shows a further summation of the integral cross sections to energetically higher electronic states according to

$$\begin{aligned}
&\sum_{n=2\text{ or }3}^{\infty}\sigma_{\text{exc.}}^{\text{DW}}(2\,^1S\rightarrow n\,^{1,3}L) \quad \text{(labeled } A\text{)},\\
&\sum_{n=2\text{ or }3}^{\infty}\sigma_{\text{exc.}}^{\text{DW}}(2\,^3S\rightarrow n\,^{1,3}L) \quad \text{(labeled } B\text{)},\\
&\sum_{n=2\text{ or }3}^{\infty}\sigma_{\text{exc.}}^{\text{DW}}(2\,^3S\rightarrow n\,^3L) \quad \text{(labeled } C\text{)},\\
&\sum_{n=2\text{ or }3}^{\infty}\sigma_{\text{exc.}}^{\text{DW}}(2\,^3S\rightarrow n\,^1L) \quad \text{(labeled } D\text{)}.
\end{aligned} \tag{12}$$

TABLE II. Sum of integral cross sections from $2\,^1S$ state (Å^2).

Energy (eV)	To all $n\,^3S$	To all $n\,^3P$	To all $n\,^3D$	To all $n\,^3L$	To all $n\,^1S$	To all $n\,^1P$	To all $n\,^1D$	To all $n\,^1L$	To all $n\,^{1,3}L$
3.00	1.46+00	6.16+00		7.62+00	1.77+01	3.33+02		3.50+02	3.58+02
4.00	8.31+01[a]	5.26+00	1.26+01	1.86+01	2.38+01	3.01+02	1.54+01	3.406+02	3.59+02
4.50	6.08−01	3.50+00	9.00+00	1.31+01	2.20+01	2.85+02	1.48+01	3.22+02	3.35+02
5.00	4.59−01	2.41+00	6.76+00	9.63+00	1.91+01	2.69+02	1.42+01	3.03+02	3.12+02
6.00	3.18+01	1.32+00	4.02+00	5.67+00	1.61+01	2.45+02	1.34+01	2.74+02	2.80+02
7.00	2.27−01	7.86−01	2.55+00	3.56+00	1.31+01	2.21+02	1.28+01	2.46+02	2.50+02
8.00	1.55−01	5.22−01	1.69+00	2.37+00	1.17+01	2.05+02	1.21+01	2.29+02	2.31+02
10.00	9.09−02	2.72−01	8.33−01	1.20+00	8.92+00	1.74+02	1.06+01	1.93+02	1.94+02
12.00	5.61−02	1.62−01	4.40−01	6.58−01	7.76+00	1.56+02	9.7+00	1.74+02	1.74+02
15.00	2.91−02	8.41−02	2.24−01	3.38−01	6.02+00	1.30+02	8.00+00	1.44+02	1.45+02
20.00	1.28−02	3.56−02	8.87−02	1.37−01	4.59+00	1.04+02	6.35+00	1.15+02	1.15+02
30.00	4.05−03	1.05−02	2.44−02	3.89−02	3.11+00	7.51+01	4.45+00	8.26+01	8.27+01
40.00	1.77−03	4.38−03	9.86−03	1.60−02	2.38+00	5.79+01	3.45+00	6.37+01	6.37+01
50.00	9.29−04	2.17−03	4.92−03	8.02−03	1.91+00	4.53+01	2.84+00	5.01+01	5.01+01
60.00	5.50−04	1.23−03	2.75−03	4.53-−03	1.60+00	3.70+01	2.42+00	4.10+01	4.10+01
81.60	2.21−04	4.85−04	1.07−03	1.78−03	1.21+00	2.61+01	1.73+00	2.91+01	2.91+01
100	1.21−04	2.59−04	5.69−04	9.49−04	9.99−01	2.10+01	1.42+00	2.34+01	2.34+01
200.00					5.35−01	8.89+00	7.16−01	1.01+01	1.01+01

[a]$8.31+01 \equiv 8.31\times10^1$.

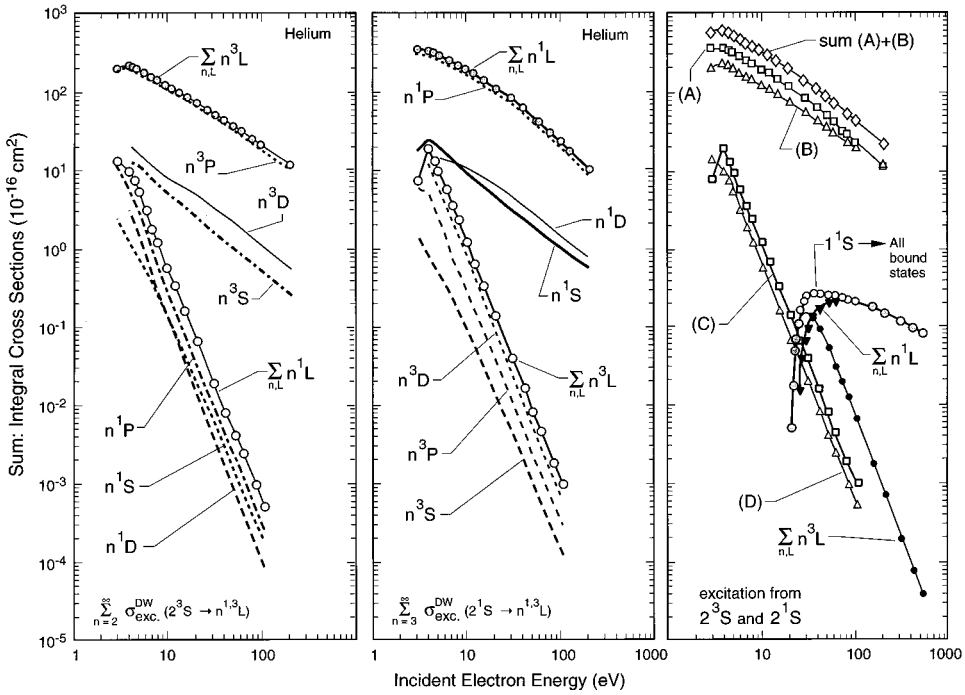

FIG. 6. Present DW approximation results for the sum of total cross sections for excitation from a given initial metastable helium state, to all final states of a specific L value. The left panel is from $2\,^3S$, and the center panel from $2\,^1S$. The right panel illustrates the further summations given in the text in Eq. (12). The total electronic excitation cross section from the $1\,^1S$ (ground) state to all excited bound states in helium is also shown in the right panel, to illustrate the relatively large magnitudes for excitation from the two metastable states.

To illustrate how much larger the electron-impact excitation cross sections from the metastable states are relative to that from the helium ground state, the right panel in Fig. 6 also shows the sum of integral cross sections from the ground state of helium to all higher bound states [1], as well as the separate sums of excitation cross sections to all singlet and triplet states. The results from this study used to generate the curves labeled (A) through (D) in Fig. 6 are also contained in Table III.

A summary comparison of those integral electron-impact excitation cross sections to bound atomic states reported here, along with other key electron collision cross sections involving metastable and ground state helium, is shown in Fig. 7, because helium appears to be the only atomic or molecular target for which all such information is known.

(i) The left panel shows various integral cross sections, for ground-state helium as the initial state: for total scattering and total ionization [15], elastic scattering [16], and excitation to all bound excited states [1].

(ii) The center panel in Fig. 7 is the same as the right panel in Fig. 6 except the curve labeled (E) represents a measure of the total cross section for production of the $2\,^3S$

TABLE III. Sum of integral cross sections from $2\,^3S$ and $2\,^1S$ state (Å^2).

Energy (eV)	$2\,^1S$ to all $n\,^3L$	$2\,^1S$ to all $n\,^1L$	$2\,^1S$ to all $n\,^{1,3}L$	$2\,^3S$ to all $n\,^1L$	$2\,^3S$ to all $n\,^3L$	$2\,^3S$ to all $n\,^{1,3}L$	$2\,^3S$, 2^1S to all $n\,^{1,3}L$
3.00	7.62+00	3.50+02	3.58+02	1.33+01	2.00+02	2.00+02	5.58+02
4.00	1.86+01[a]	3.40+02	3.59+02	9.67+00	2.16+02	2.25+02	5.84+02
4.50	1.31+01	3.22+02	3.35+02	7.30+00	2.03+02	2.13+02	5.48+02
5.00	9.63+00	3.03+02	3.12+02	5.39+00	1.90+02	1.96+02	5.08+02
6.00	5.67+00	2.74+02	2.80+02	3.14+00	1.68+02	1.71+02	4.51+02
7.00	3.56+00	2.46+02	2.50+02	1.78+00	1.52+02	1.54+02	4.04+02
8.00	2.37+00	2.29+02	2.31+02	1.21+00	1.40+02	1.41+02	3.72+02
10.00	1.20+00	1.93+02	1.94+02	5.63−01	1.21+02	1.21+02	3.16+02
12.00	6.58−01	1.74+02	1.74+02	3.34−01	1.06+02	1.07+02	2.81+02
15.00	3.38−01	1.44+02	1.45+02	1.60−01	9.12+01	9.13+01	2.36+02
20.00	1.37−01	1.15+02	1.15+02	6.60−02	7.38+01	7.39+01	1.89+02
30.00	3.89−02	8.26+01	8.27+01	1.92−02	5.40+01	5.40+01	1.37+02
40.00	1.60−02	6.37+01	6.37+01	8.04−03	4.28+01	4.28+01	1.07+02
50.00	8.02−03	5.01+01	5.01+01	4.08−03	3.55+01	3.55+01	8.56+01
60.00	4.53−03	4.10+01	4.10+01	2.40−03	3.04+01	3.04+01	7.15+01
81.60	1.78−03	2.91+01	2.91+01	9.32−04	2.33+01	2.33+01	5.24+01
100.00	9.49−04	2.34+01	2.34+01	5.04−04	1.96+01	1.96+01	4.31+01
200.00		1.01+01	1.01+01		1.14+01	1.14+01	2.16+01

[a] $1.86+01 \equiv 1.86\times10^1$.

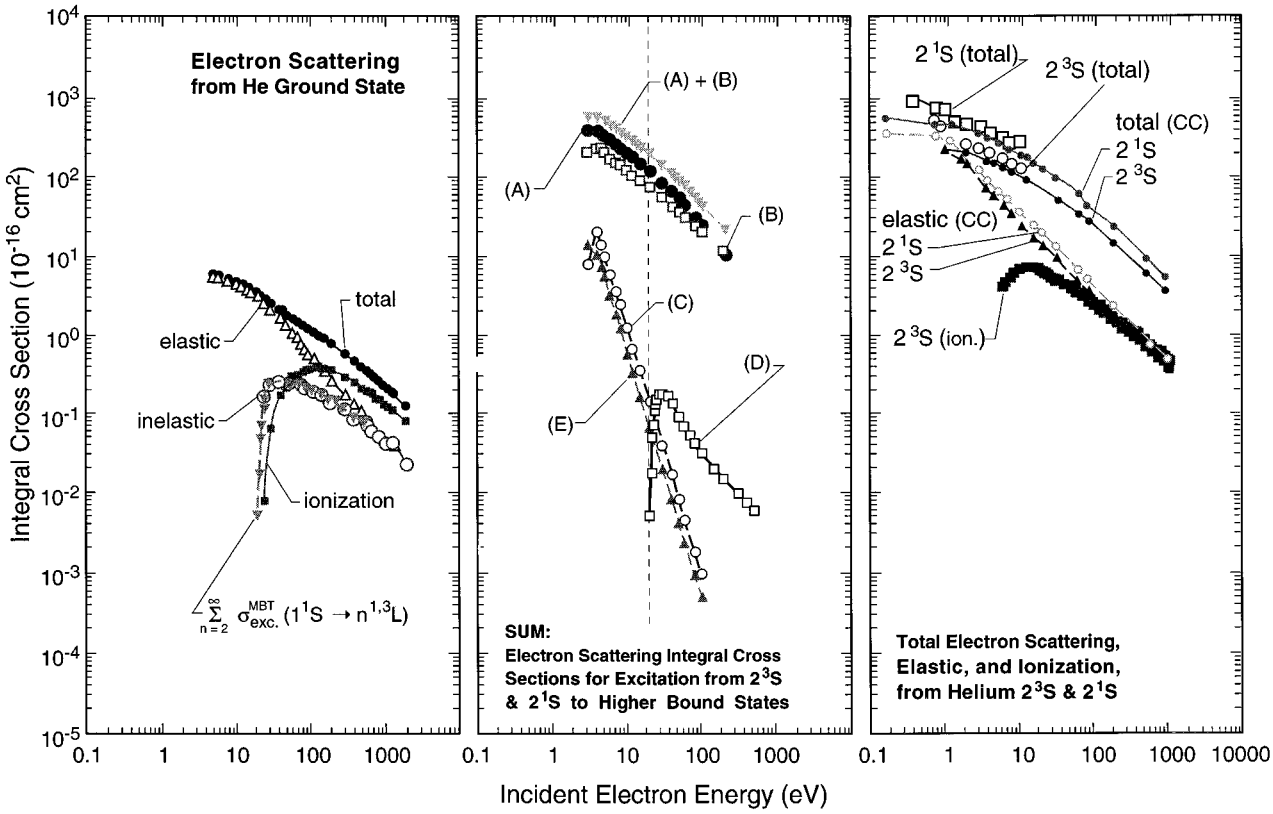

FIG. 7. Summary of key integral cross sections for electron scattering by atomic helium in the ground and two metastable electronic states. Left panel: integral cross sections for elastic scattering, ionization, total scattering, and for excitation to all bound states from *ground-state* helium. Center panel: sum of integral excitation cross sections to all higher bound states from the $2\,^3S$ and $2\,^1S$ states is shown separately. The definitions of the curves are given in Eq. (12). The curve labeled E denotes an estimate of the cross section for production of the metastable $2\,^3S$, $2\,^1S$ states by electron impact [see text and Eq. (12)]. The light vertical dashed line denotes the lowest-energy excitation threshold for ground-state helium. Right panel: additional integral cross-section information for electron collision processes involving the two helium metastable states which are included here for completeness. See text for details.

and $2\,^1S$ metastable states according to the definition

$$\sigma(E)=\sum_{n=2}^{\infty}\sigma_{\text{exc.}}^{\text{MBT}}(1\ ^1S\rightarrow n\ ^3L)+\sigma_{\text{exc.}}^{\text{MBT}}(1\ ^1S\rightarrow 2\ ^1S)$$
$$=(\text{net production of } 2\ ^3S)$$
$$+(\text{direct production of } 2\ ^1S), \qquad (13)$$

where the cross-section data were taken from the work of Cartwright *et al.* [1] and Trajmar *et al.* [2]. The point of showing this panel is to illustrate how much larger the cross sections for excitation from the two metastable states are than that for total production of the two metastable states.

(iii) The right panel in Fig. 7 is a summary of additional key integral cross-section data for electron collisions involving the $2\,^3S$ and $2\,^1S$ states. The curves labeled ''elastic CC'' and ''total CC'' are from the recent ''convergent close-coupling'' work of Bray and Fursa [11]. The data illustrated in Fig. 7 are also given in Table III.

It is important to recognize the practical significance of the magnitudes and energy dependence of the integral collision cross sections for excitation from the two helium metastable states shown in Fig. 7. Specifically, electron collisions with metastable helium atoms should be expected to play an important role in a partially ionized helium plasma environment for the following reasons.

(i) The magnitudes of the integral cross sections for elastic scattering, excitation, and ionization involving the two metastable states are a factor of 100, or more, greater than that for ground-state helium (shown in Fig. 7).

(ii) The energy threshold for excitation and ionization from the metastable states are at a few eV compared to about 20 eV for the ground state (the vertical line, center panel, Fig. 7). In most partially ionized plasma there are orders of magnitude more electrons at low energy than above the ionization threshold.

ACKNOWLEDGMENTS

The authors thank Igor Bray, Flinders University, for providing the results of his CC calculations (Ref. [11]) prior to publication, and for many stimulating discussions. This work was performed under the auspices of the U.S. Department of Energy.

[1] D. C. Cartwright, G. Csanak, S. Trajmar, and D. F. Register, Phys. Rev. A **45**, 1602 (1992).
[2] S. Trajmar, D. F. Register, D. C. Cartwright, and G. Csanak, J. Phys. B **25**, 4889 (1992).
[3] D. C. Cartwright and G. Csanak, Phys. Rev. A **51**, 454 (1995).
[4] G. Csanak, H. S. Taylor, and R. Yaris, Phys. Rev. A **3**, 1322 (1971).
[5] G. Csanak, D. C. Cartwright, and F. J. da Paixao, Phys. Rev. A **48**, 2811 (1993).
[6] M. Cohen and R. P. McEachran, Proc. Phys. Soc. **92**, 37 (1967).
[7] R. P. McEachran and M. Cohen, J. Phys. B **2**, 1271 (1969).
[8] Y. K. Kim and M. Inokuti, Phys. Rev. **181**, 205 (1969).
[9] R. Muller-Fiedler, P. Schlemmer, K. Jung, H. Hotop, and H. Ehrhardt, J. Phys. B **17**, 259 (1984).
[10] R. B. Lockwood, F. A. Sharpton, L. W. Anderson, and C. C. Lin, Phys. Lett. A **166**, 357 (1992).
[11] I. Bray and D. V. Fursa, J. Phys. B **28**, L197 (1995); see also F. J. de Heer *et al.*, Nucl. Fusion Suppl. **6**, 7 (1996).
[12] M. R. Flannery and K. J. McCann, Phys. Rev. A **12**, 846 (1975).
[13] E. J. Mansky and M. R. Flannery, J. Phys. B **25**, 1591 (1992).
[14] W. C. Fon, K. A. Berrington, and A. E. Kingston, J. Phys. B **24**, 2161 (1991).
[15] S. Trajmar and J. C. Nickel, Adv. At. Mol. Opt. Phys. **30**, 45 (1993).
[16] I. Shimamura, Sci. Papers Inst. Phys. Chem. Res. **82**, 1 (1989).